Development of Ganoderma lucidum spore powder based proteoglycan and its application in hyperglycemic, antitumor and antioxidant function

and antioxidant function

Li-Fang Zhu,[1, 2] Yuanfa Yao,[1, 2] Zeeshan Ahmad,[3] Ming-Wei Chang[1, 2, 4*]

[1] Key Laboratory for Biomedical Engineering of Education Ministry of China, Zhejiang University, Hangzhou, 310027, PR China.

[2] Zhejiang Provincial Key Laboratory of Cardio-Cerebral Vascular Detection Technology and Medicinal Effectiveness Appraisal, Zhejiang University, Hangzhou, 310027, PR China.

[3] Leicester School of Pharmacy, De Montfort University, The Gateway, Leicester, LE1 9BH, UK.

[4] Nanotechnology and Integrated Bioengineering Centre, University of Ulster, Jordanstown Campus, Newtownabbey, BT37 0QB, Northern Ireland, UK.

*corresponding author: Ming-Wei Chang, Ph.D., Assoc. Professor

Tel: +86(0)571-87951517, Email: mwchang@zju.edu.cn

obtained via solvent extraction and optimized using response surface methodology (RSM). The differences among the characteristics of the new proteoglycan from cracked (proteoglycan-C) and uncracked GLSP (proteoglycan-UC) were explored. The SDS-PAGE results showed the molecular weight of protein contained in proteoglycan-UC (55, 72, 95 kDa) was different to that proteoglycan-C (43, 95 kDa). The differences of these amino acids (Glu, Arg, Leu and Lys) content and monosaccharides (Fuc, Gal, Glc, Man and Gal-AC) content between proteoglycan-C and proteoglycan-UC were determined by HPLC/ ion chromatography. The 2,2'-azino-bis (3-ethylbenzthiazoline-6-sulphonic acid) (ABTS) and 1,1-Diphenyl-2-picrylhydrazyl (DPPH) radical scavenging activities of proteoglycan-C were higher than that proteoglycan-UC. The proteoglycan-UC exhibited stronger hypoglycemic and antibacterial effects against *E. coli* and *S. aureus*, and the proteoglycan-C and proteoglycan-UC showed antitumor effects with potential for therapeutic applications.

Keywords: proteoglycan; *Ganoderma lucidum* spore powder; hypoglycemic; antibacterial; antitumor.

effects and minor side effects of the products in prevention and alleviation of cancer, hypertension and diabetes [1]. For example, Lentinan, a polysaccharide obtained from the stipe portion of *Lentinus edodes* mushroom, revealed anticancer activities against human colon cancer [2]. In addition, the proteoglycan obtained from *Ganoderma lucidum* (*G. lucidum*) fruiting bodies has demonstrated protective effects on the kidneys and amelioration of diabetic nephropathy [3].

G. lucidum is a well-known traditional Chinese medicine herb that has been used to promote health and longevity for several thousands of years [4]. During the past few decades, applications of *G. lucidum* have been explored and include alleviating symptoms of asthma [5], promoting wound healing [6], as antitumor agents [7] and also as an oral multidrug [8, 9]. Among the bioactive ingredients, the proteoglycans and polysaccharides have shown important roles in medicinal potencies [10]. The proteoglycan is a kind of glycoprotein consisting of a core protein linked to one or more glycosaminoglycan chains via covalent bonding [11], and shows efficient hypoglycemic activity in vitro [12] as well as excellent anti-herpetic activities against type 1 and type 2 herpes simplex virus has been revealed [13]. This suggests the polysaccharides presence during the extraction of protein is advantageous with regards to the bioactive effects of the proteoglycan.

firstly confirmed. The differences between physicochemical properties, amino acid, and monosaccharide in cracked GLSP and uncracked GLSP were then explored through Fourier transform infrared spectroscopy (FTIR), High Performance Liquid Chromatography (HPLC) and ion chromatography. Subsequently, the antioxidant, antitumor and antibacterial effects of proteoglycan from cracked and uncracked GLSP were compared. In consideration of the widespread applications of proteoglycans and *G. lucidum*, the results in this study may broaden the source of proteoglycans and application of GLSP.

2. Materials and methods

2.1 Materials

GLSP (cracked and uncracked wall) was offered by TianHe Agricultural Group (ZheJiang LongQuan, China). Sodium hydroxide (troche), ammonium sulfate (powder), methanol, absolute ethanol and hydrochloric acid were purchased from Sinopharm Chemical Reagent Co., Ltd (Shanghai, China). Fetal bovine serum (FBS) was purchased from Sijiqin (Sijiqin, Hangzhou, zhejiang, China), Dulbecco's modified eagle's medium (DMEM) was purchased from Gibico (Gibco, USA) and deionized water (DI) were offered by the Millipore Milli-Q Reference ultrapure water purifier

electrophoresis (SDS-PAGE) Gel Quick Preparation Kit were offered by Shanghai Beyotime biotechnology Co., Ltd (Shanghai, China). Violet red bile agar, baird-parker agar base, adding egg-yolk tellurite emulsion, nutrient broth, 7.5% sodium chloride broth were from Qingdao Hope Bio-Technology Co., Ltd (Shandong, China). Universal indicator paper (pH 1-14, Shanghai SSS reagent Co., Ltd). All chemicals were analytical grade with no further purification before experimentation.

2.2 Extraction of proteoglycan

The proteoglycan was obtained using conventional water extraction via a water bath (DZKW-D-4, Suzhou Jiangdong precise instrument Co., Ltd, Suzhou, China). Approximately 1g of dried GLSP (uncracked) was dispersed with DI water according to a predetermined solid-to-liquid ratio, and then kept in the water bath at the predetermined temperature for predetermined time. The mixture was then centrifuged at 8000 rpm, at 4 ℃ for 30 min using Centrifuge 5810 R (Eppendorf, Germany), according the method in previous work [14]. The supernatant was collected and concentrated using Rotavapor (RE-52A, Shanghai, China) at -0.09 MPa and 55 ℃ to one-tenth of the volume. Ammonium sulfate was introduced to the concentrated mixture until saturation. NaOH was introduced to achieve a neutral pH and left to stand

protein assay reagent (Bio-Rad, USA). Since proteoglycan is similar to glycoprotein and there is no single standard for proteoglycan, BSA was used as a standard protein. Absorbance of BSA was examined at 595 nm using UV spectrophotometer (UV-2600, Shimadzu, Japan). The standard curve of concentration-absorbance was plotted (in Fig. S1), and fitting equation is shown in Eq. (1):

$$y = 9.1755x + 0.011 \quad (1)$$

where, y was the absorbance, x was the concentration (mg/mL).

Box-behnken design was used to optimize the extraction parameters according to the results from response surface methodology (RSM) (Design-Expert 8.0.6 Trial, Stat-Ease, Inc. USA). Four three-level independent variables (Table S1) were selected based on the single factorial assays.

2.3 Molecular weight determination of protein

The protein molecular weight was determined using Sodium Dodecyl Sulfate Polyacrylamide Gel electrophoresis (SDS-PAGE) [16]. Each sample (20 μL, 10 mg/mL) was determined in SDS-PAGE with a 6% resolving gel and a 5% stacking gel (SDS-PAGE Gel Quick Preparation Kit). The operation was performed at 100 V through stacking gel followed by 120 V to the end of resolving gel using Power Pac™ Basic

The proteoglycans were determined using Fourier transform infrared (FT-IR) spectroscopy (IR Affinity 1, Shimadzu, Japan). The samples were grounded with KBr powder and then pressed into pellet using powder compressing machine (FW-4A, Tianjin TUOPU instrument Co., Ltd, Tianjin, China) under the pressure ~14 MPa for 2 min, and getting the spectrum with 20 scans at a resolution of 4 cm^{-1} (4000–400 cm^{-1}).

2.5 Amino acid and monosaccharide composition of proteoglycan

The amino acid content of the protein was determined using a High Performance Liquid Chromatography system (HPLC, UitMate 3000, Thermo-Fisher Scientific, USA), which was equipped with a DAD-3000 (RS) fluorescence detector. The analyte was separated using an analytical column ZORBAX Eclipse-AAA (4.6 mm×150 mm, Agilent ZORBAX Eclipse, Agilent Technology, USA). The mobile phase consisted of Na_2HPO_4 (pH 7.8) with a concentration of 40 mM and acetonitrile-methanol-DI (45: 45: 10, v/v/v).

The monosaccharide was detected using an ion chromatograph system (Dionex ICS-5000, Thermo-Fisher Scientific Dionex, USA) combining a chromatographic guard column (3 mm×50mm, Dionex Carbo PAC^{TM} PA20) and anion exchange column (3 mm×250 mm, Dionex Carbo PAC^{TM} PA20). The ICS-5000 electrochemical detector

The ABTS radical scavenging activity was determined using a total antioxidant capacity assay kit. In brief, the ABTS radical solution and trolox standard solution with various concentrations (0.1, 0.2, 0.4, 0.6, 0.8, 1.0 mM) were prepared according to manufacturer instructions. Peroxidase stock solution was added to a 96-well plate (20 μL/well). DI water was used as blank control, trolox standard solution was added for the positive control and sample solution was added for the sample group (10 μL/well). Following that, ABTS radical solution was added (170 μL/well) and the plate was cultured for 6 minutes at 25°C. The absorbance was measured at 414 nm using Spectra Max 190 microplate reader (NanoDrop, USA). The antioxidant activity of sample was shown as Trolox equivalent antioxidant capacity (TEAC) and calculated as Eq. (2), according to previous works [14, 17] :

$$\text{TEAC (mM Trolox/ mg protein of sample)} = \frac{A_s - A_b}{A_b} \times \frac{1}{mX} \quad (2)$$

Where, the A_s is the absorbance of sample; the A_b is the absorbance of blank control; the m is slope of a plot between antioxidant capacity and mM Trolox; the X is mg protein of sample.

The DPPH radical scavenging activity was measured using the previous method of Yang et al. [18]. Using DI water and ethanol to dissolve proteoglycan and DPPH, to the final concentration of 100 μg/mL and 0.2 mM, respectively. Mixing 1 mL sample

DPPH radical scavenging activity (%) = $[1-(A_s-A_c)/A_b]\times 100\%$ (3)

Where, the A_s is the absorbance of sample solution; the A_c is the absorbance of control, which the DPPH was replaced by ethanol in equal volume; the A_b is the absorbance of blank, which the sample solution was replaced by DI water in equal volume.

2.7 Hypoglycemic activity assay in vitro

2.7.1 Hypoglycemic effect on normal HepG2 cells

HepG2 (human hepatocellular liver carcinoma) cells (ca. 1.4×10^5 cells/mL) were cultured in DMEM supplemented with 10% FBS and 1% penicillin-streptomycin in cell culture dishes (diameter, Φ= 6 cm) under standard conditions (37 °C, 5% CO_2) for 48 h. Then, pipetted cell suspensions into a 96-well plate (100 μL/well) and incubated in serum-free DMEM at standard conditions for 12 h. Following this, cells for blank control were incubated in serum-free DMEM, and cells for positive control were incubated in serum-free DMEM supplemented with metformin (1×10^{-3}mol/L). The treatment groups were incubated in serum-free DMEM supplemented with various concentrations of proteoglycan (0.1, 1, 10 mg/mL). After being incubated 24 h, measuring the glucose content of supernatant of media using Micro Blood Sugar

HepG2 cells (ca. 1.4×10^5 cells/mL) were seeded into a 12-well plate for 24 h in serum-free DMEM. The cells were then treated with serum-free DMEM with insulin (1×10^{-7}mol/L) for 1 h. Subsequently, the cells were incubated in serum-free DMEM with metformin (1×10^{-3}mol/L) or various concentrations of proteoglycan (1, 5, 10mg/mL) for 24 h. Finally, the glucose content of supernatant of media was measured by using UV-Vis.

2.8 Antitumor activities assay *in vitro*

2.8.1 Cell viability assay

The antitumor effects of proteoglycan on tumor cell lines were determined using CCK-8 (cell counting Kit-8 reagent, Dojindo Laboratories, Kumamoto, Japan) assay [20]. In brief, HeLa cell suspension (ca. 1.4×10^5 cells/mL) was obtained after being cultured in DMEM supplemented with 10% FBS and 1% penicillin-streptomycin in cell culture dishes (Φ = 6 cm) under standard conditions for 48 h. 100 μL cell suspensions were pipetted into a 96-well plate and incubated at standard conditions for 24 h. For treatment group, 100 μL each well of proteoglycan solution was added after being disinfected using UV radiation for 4 h; and 100 μL medium was added to the control. After being cultured for 24 h, the cells were added 10 μL CCK-8 solution and the

blank group, respectively.

2.8.2 AO/EB staining

HeLa cells were stained using AO/EB dye mixture. In brief, cell suspension (1.4×10^5 cells/mL) were seeded into a 6-well plate. After being incubated 24 h for adherence, the cells were treated with proteoglycan solution with various concentrations (1 or 5 mg/mL) for another 48 h. 20 μL of AO/EB dye mixture (100μg/mL EB and 100 μg/mL AO into the 6-well plate and left to stand for 30 min at 37°C. The plate was analyzed using fluorescence microscopy (Olympus, BX61W1-FV1000, Tokyo, Japan).

2.9 Antibacterial activity assay

The antibacterial effects of proteoglycan on *E. coli* (NW1014 (8099), Nanjing Maojie Microbiology Technology Co., Ltd, Jiangsu, China) and *S. aureus* (CMCC(B)26003, Shanghai Luwei Microbial SCI. & TECH. Co., Ltd, China) was studied using the method [22]. Pressing proteoglycan powder (ca. 100 mg) to a disk by the powder compressing machine. Coating 0.2 mL (1.2×10^6 CFU/mL) inoculums of *E. coli* and *S. aureus* on violet red bile agar and baird-parker agar base plates adding egg-yolk tellurite emulsion, respectively. Then, put the agar plate (Φ≈3 cm) in biochemical

Meanwhile, 0.01 mL (ca. 1.2×10^6 CFU/mL) inoculum of *E. coli* and *S. aureus* was added into 100 mL nutrient broth and 7.5% sodium chloride broth respectively, and then incubated in the biochemical incubator at 37℃for 24h. After that, using 25 μg/mL FDA and PI to stain the bacteria for 20 min at 25℃and was kept away from light. The fluorescence value was measured using a fluorescence microplate reader (FlexStation II, NanoDrop, USA), and the fluorescence value was calculated using previous method [22].

2.10 Statistical analysis

All experiments were performed in triplicate and data is given as mean ± standard deviation (n=3). Statistical analysis was performed using SPSS software (SPSS Statistics v18, IBM, UK). The one-way analysis of variance (ANOVA) were revealed using RSM (Design- Expert 8.0.6 Trial, Stat-Ease, Inc., USA). All the statistical plots were plotted using Origin software (OriginLab, USA).

3. Results and discussion

3.1 Optimization of the proteoglycan extraction

This study of controlling parameters (e.g. time, temperature, extraction times, solid-

effects on yields. The experimental data and results are shown in Table S2. Then, the regression equation was obtained according to the results of ANOVA:

$$Y=3.93+0.027\times A-0.044\times B+0.044\times C+0.12\times D-0.20\times A\times B+0.099\times A\times C+0.079\times A\times D-0.12\times B\times C+4.75\times B\times D\times 10^{-3}-0.24\times C\times D-0.63\times A^2-0.78\times B2-0.94\times C^2-0.88\times D^2 \quad (5)$$

where, Y is the proteoglycan yield (%) in the resultant product probably; A, B, C and D was the solid-liquid ratio, time, temperature and pH value, respectively.

The RSM results (Fig. 1 & Fig. S3) revealed the interactions among the experimental parameters. As the results shown (Table S3), the fitting model F-value was 3.23 and p-value was 0.024 (< 0.05), which revealed the quadratic model was significant. The linear coefficients (A, B, C, D), cross product coefficients (AB, AC, AD, BC, BD, CD) were found insignificant ($p > 0.05$), whereas the quadratic coefficients (A^2, B^2, C^2, D^2) exhibited significant effect ($p < 0.05$). The significant order priority of the four factors on the result was pH value > time = temperature>solid-liquid ratio, which confirmed the fact that the little longer extraction time [24] with appropriate temperature [25], and neutral pH [26] may be improved protein extraction.

After calculations, the predictive maximum protein yield (4.525%) was obtained on the optimizing parameters: 1:40 (g: mL), 2.93 h, 35.19 ℃ and 10.07 (pH value). For

optimizing extraction parameters of proteoglycan.

Then, the difference in physicochemical properties, amino acid, and monosaccharide content of the proteoglycan from cracked well GLSP (proteoglycan-C) and uncracked well GLSP (proteoglycan-UC) were explored through FTIR, HPLC and Ion chromatography. Following that, the antioxidant, antitumor and antibacterial effects of proteoglycan-C and proteoglycan-UC were compared.

3.2 FT-IR analysis

FT-IR is frequently used to analyze functional groups of a compound [27-29]. The FT-IR spectra of proteoglycan-C and proteoglycan-UC are presented in Fig. 2a. The peaks at 1527 and 1664 cm^{-1} were due to the presence of amide II and amide I respectively, which revealed the isolated compound contained protein fractions [30]. The signals at 2920, 2850, 1478, 1160, 1078 cm^{-1} were attributed to the presence of pyranose ring [31]. Moreover, the absorption peaks around 2920, 1620 and 1400cm^{-1} were the characteristic absorption peaks of polysaccharide [32] due to C-H and –COOH groups, respectively [24]. The FT-IR results confirmed that the isolated proteoglycan was a polysaccharide and protein complex. Also, there were no obvious differences in the functional group between the proteoglycan from cracked and uncracked GLSP; just

303 stained using Coomassie brilliant blue, which revealed the protein was a non-
304 monomeric protein. Comparing with standard protein molecular weight marker (lane
305 1), the molecular weight of protein in proteoglycan-C (lane 2-4) was 43 and 95 kDa;
306 and the protein contained in proteoglycan-UC (lane 5-7) possessed molecular weight
307 as follows: 55, 72 and 95 kDa. The band width of protein with molecular weight 95
308 kDa of proteoglycan-UC (lanes 5-7) is wider than that of proteoglycan-C (lanes 2-4),
309 which indicates proteoglycan-UC contains a higher protein content than proteoglycan-
310 C. The protein obtained in this work was consistent with the protein with molecular
311 range 12 to 150 kDa from *Ganoderma boninense* [33].
312
313 **3.4 Amino acid content and constitution of polysaccharide**
314 The amino acid content of proteoglycan was determined using HPLC (Fig. 3a & b).
315 The content of amino acids (e.g. Asp, Glu, Lys) were calculated (Table S4). The Arg
316 content of proteoglycan-UC (10.74%) was did not appeared in proteoglycan-C; the
317 content of Lys in proteoglycan-C (6.32%) was not detected in proteoglycan-UC. The
318 Asn and Gln were not detected in proteoglycan-C and proteoglycan-UC.
319 The monosaccharide contained in proteoglycan was determined using Ion
320 chromatograph system. The results (Fig. 3c & d) revealed the presence of several kinds

proteoglycan-C. Besides, the Glc and Man contents of proteoglycan-UC (524.281, 6.386 μg/mg, respectively) were more than twice of that proteoglycan-C (247.959, 2.667 μg/mg, respectively). While the Fuc and Gal content of proteoglycan-UC was 1.186 μg/mg and 7.421μg/mg respectively, higher content was found in proteoglycan-C (3.308 μg/mg and 13.320 μg/mg, respectively). The Xyl, Fru, Rib and Glc-AC were not detected in proteoglycan-C and proteoglycan-UC. The results confirmed that the effect of GLSP (cracked or uncracked) on the monosaccharide content was significant. Differences in amino acid and monosaccharide content of proteoglycan between cracked and uncracked wall GLSP may be attributed to two main causes. The first is oxidation reactions which occur in cracked wall GLSP. Secondly, Maillard reaction between monosaccharides and amino acids influence ion chromatography detection. The latter can also occur (and impact) during ion chromatography experimental conditions [34].

3.5 Free radical scavenging activity

The scavenging effect of ABTS was expressed as Trolox equivalent antioxidant capacity (TEAC), as shown in Fig. 4. The ABTS scavenging activity of proteoglycan-C and proteoglycan-UC (1 mg/mL) was 73.3±6.7% and 47.2±5.9%, respectively while

C was higher than that of proteoglycan-UC, which was the same for both ABTS and DPPH test. The differences among these amino acid contents might be the key causes responsible for the antioxidant activities differences of the proteoglycans as the peptides contained in the amino acids (His, Phe and Pro) (Tables S4 & S5) have shown antioxidant activity [35].

3.6 Hypoglycemic activity *in vitro*

Metformin is used for the treatment of type 2 diabetes, and is a commercially available hypoglycemic drug [36]. Numerous studies have used this drug to demonstrate hypoglycemic activity, typically as a positive control when examining hypoglycemic effects between various treatment groups. Therefore, metformin was selected to compare hypoglycemic activity of proteoglycan in the current work. The glucose concentration of the supernatant of media after being cultured for 24 h indicated the capacity of glucose consumption of HepG2 cell. The hypoglycemic potency of proteoglycan on normal HepG2 cells is shown in Fig. 5a. The glucose concentration in the proteoglycan treatment (10 mg/mL) was comparable with the metformin treatment group (10^{-3} mol/L). Differences in hypoglycemic effect on normal HepG2 cells between treatment and control groups was not significant. This may be due to normal HepG2

proteoglycan-C was stronger than proteoglycan-UC, and indicates proteoglycan (concentration of 10 mg/mL) exhibits a similar hypoglycemic effect as metformin at a concentration of 10^{-3} mol/L on normal HeG2 cells.

The hypoglycemic effect of proteoglycan on insulin-induced insulin resistance type HepG2 cells, which used to imitate T2DM patients [12] is shown in Fig. 5b. The glucose concentration in insulin treatment group (10.91 ± 0.56 mM) was comparable with that of control (10.92±0.18 mM), indicating that the insulin-induced insulin resistance type HepG2 cells were constructed successfully. Comparing with control, the hypoglycemic effect of resulting proteoglycan-C and proteoglycan-UC on insulin resistance type HepG2 cells were obvious, for the P- < 0.05 (p- value was 0.03 and 0.02, respectively). Furthermore, the glucose concentration treated by proteoglycan-C was little lower than that of proteoglycan-UC.

The mechanism under the hypoglycemic effect of the proteoglycan is most likely an interaction between proteoglycan and protein tyrosine phosphatase 1B (PTP1B), which was inhibited via interactions between the carboxyl groups of Asp and Glu and Tyr20, Arg24 and Arg254 active sites of PTP1B [37]. Thus, the differences of Asp and Glu content (Table S4) in proteoglycan-C and proteoglycan-UC were the major causes for the difference in hypoglycemic activity.

antitumor activity *in vitro* [16, 38]. As shown in Fig. 6a, the HeLa cell viability decreased as treatment dose and time increases. When HeLa cells were treated with 0.5 or 1.0 mg/mL of proteoglycan-C for 12 h, the cell viability was 95.2 ± 1.5% and 72.5 ± 1.9%, respectively, and decreased further (to 69.9 ± 2.6% and 62.3 ± 0.9%) at the treatment of 48 h. The result of proteoglycan-UC on the cell viability was 90.3 ± 0.9% and 78.2 ± 5.3% for 0.5 or 1.0 mg/mL for 12 h, respectively, and then decreased to 69.1±1.0% and 58.2 ± 0.9% when treated for 48 h, respectively.

The antitumor effect can be visualized via AO/EB dual staining results (Fig. 6). The blank control (Fig. 6b) presented bright green with slight orange fluorescence, indicating most vital cells. At the treatment of proteoglycan-C or proteoglycan-UC (1.0 mg/mL) (Fig. 6b1 & c1), the green fluorescence was weaker and orange fluorescence was brighter, while little less orange fluorescence showed with lower concentration (0.5 mg/mL) treatment (Fig. 6b2 & c2). This indicates the number of viable cells was less than that of the control and the number of necrotic cells had increased; consistent with previously reported studies [39]. The results confirmed the antitumor activity of proteoglycan, which probably due to the polysaccharide fraction in proteoglycan can stimulate the immune system [40] or suppress the cell growth by inhibiting the activity of Akt and transcription factors AP-1 and nuclear factor-kappa B (NF-κB) [41] .

Compared to control, the proportion of viable cells for *E. coli* decreased to 89.6 ± 9.9% and the necrotic cells proportion increased to 112.5 ± 9.1% (Fig. 7a) at the treatment of proteoglycan-C (1mg/mL). The proportion of viable and necrotic cells of was 93.6 ± 9.2% and 107.5 ± 3.9% respectively when *E. coli* was treated with proteoglycan-UC (1mg/mL). For *S. aureus* (Fig. 7b), at the treatment of proteoglycan-C (1 mg/mL), the proportion of viable and necrotic cells was 90.8 ± 8.7% and 124.9 ± 6.5% respectively. The same treatment of proteoglycan-UC induced the proportion of viable and necrotic cells was 97.5 ± 5.4% and 108.4 ± 7.1% respectively. Thus, these results indicate the antibacterial activities against *E. coli* and *S. aureus* of proteoglycan-UC were stronger than proteoglycan-C.

The antibacterial properties can be visualized using disk diffusion method [42]. Figs. 7 c1-d2 presents a clear inhibition zone with agar plates coated with *E. coli* and *S. aureus*. The diameter of inhibition zone for *S. aureus* is larger than that for *E. coli* (Table 1). The difference in activity is attributed to the bacterial cell type. *S. aureus* is Gram-positive bacteria and restricting entry of nutrients into cells leads to death. *E. coli* is Gram-negative bacteria and an increase in cell permeability results in death [43]. This is the same case for both proteoglycan-C and proteoglycan-UC, which was consistent with previous works [44]. The probable mechanism was that binding of polysaccharides

4. **Conclusion**

In summary, the proteoglycan from GLSP was obtained using conventional water extraction. The extraction parameters were optimized through RSM results. The results revealed that the proteoglycan obtained from cracked and uncracked GLSP differed its characteristics with respect to molecular weight, amino acid content, monosaccharide content and antibacterial activity. The proteoglycan-C (from cracked GLSP) possessed smaller molecular weight, higher content amino acid of Lys and monosaccharide of Gal comparing with that proteoglycan-UC (from uncracked GLSP). Moreover, the proteoglycan-UC contained higher content amino acids of Arg, Glc, monosaccharide of Man, and revealed stronger antibacterial effects against *E. coli* and *S. aureus* and stronger hypoglycemic effect in vitro than that of proteoglycan-C. Meanwhile, the proteoglycan-C exhibited stronger scavenging effects against ABTS and DPPH radicals. The antitumor effects against HeLa cells of proteoglycan-C were similar to that of proteoglycan-UC. Overall, the obtained results regarding antioxidant, hypoglycemic, antitumor and antibacterial activity revealed that the resulting proteoglycan from GLSP is useful as a functional additive as well as a potential candidate for a therapeutic agent.

457 (2017QNA5017), the Major Scientific Project of Zhejiang Lab (No. 2018DG0ZX01)
458 and Key Technologies R&D Program of Zhejiang Province (2015C02035).

459

460 **Competing interests**

461 There are no conflicts of interests to declare.

462

[2] Y. Wang, G. Xu, X. Tang, H. Chen, Polysaccharide lentinan extracted from the stipe of Lentinus edodes mushroom exerts anticancer activities through the transcriptional regulation of cell cycle progression and metastatic markers in human colon cancer cells, The FASEB Journal 31(1_supplement) (2017) lb391-lb391.
[3] D. Pan, D. Zhang, J. Wu, C. Chen, Z. Xu, H. Yang, P. Zhou, A novel proteoglycan from Ganoderma lucidum fruiting bodies protects kidney function and ameliorates diabetic nephropathy via its antioxidant activity in C57BL/6 db/db mice, Food. Chem. Toxicol. 63 (2014) 111-118.
[4] C. Zhao, C. Zhang, Z. Xing, Z. Ahmad, J.-S. Li, M.-W. Chang, Pharmacological effects of natural Ganoderma and its extracts on neurological diseases: A comprehensive review, Int. J. Biol. Macromol. 121 (2019) 1160-1178.
[5] Z. Xing, C. Zhang, C. Zhao, Z. Ahmad, J.-S. Li, M.-W. Chang, Targeting oxidative stress using tri-needle electrospray engineered Ganoderma lucidum polysaccharide-loaded porous yolk-shell particles, Eur. J. Pharm. Sci. 125 (2018) 64-73.
[6] C. Zhang, Y. Li, Y. Hu, Y. Peng, Z. Ahmad, J.-S. Li, M.-W. Chang, Porous Yolk–Shell Particle Engineering via Nonsolvent-Assisted Trineedle Coaxial Electrospraying for Burn-Related Wound Healing, ACS Applied Materials & Interfaces 11(8) (2019) 7823-7835.
[7] C.J. Weng, C. Chifai, Y. Gowchin, J.W. Liao, D.H. Chen, K.D. Chen, Inhibitory effects of Ganoderma lucidum on tumorigenesis and metastasis of human hepatoma cells in cells and animal models, J. Agric. Food. Chem. 57(11) (2009) 5049-57.
[8] S. Wu, J.-S. Li, J. Mai, M.-W. Chang, Three-Dimensional Electrohydrodynamic Printing and Spinning of Flexible Composite Structures for Oral Multidrug Forms, ACS Applied Materials & Interfaces 10(29) (2018) 24876-24885.
[9] L.-F. Zhu, X. Chen, Z. Ahmad, J.-S. Li, M.-W. Chang, Engineering of Ganoderma lucidum polysaccharide loaded polyvinyl alcohol nanofibers for biopharmaceutical delivery, J. Drug. Deliv. Sci. Technol. 50 (2019) 208-216.
[10] S. Zhang, S. Nie, D. Huang, W. Li, M. Xie, Immunomodulatory effect of Ganoderma atrum polysaccharide on CT26 tumor-bearing mice, Food. Chem. 136(3-4) (2013) 1213-1219.
[11] M.-F. Moradali, H. Mostafavi, S. Ghods, G.-A. Hedjaroude, Immunomodulating and anticancer agents in the realm of macromycetes fungi (macrofungi), Int. Immunopharmacol. 7(6) (2007) 701-724.
[12] Z. Yang, F. Wu, H. Yang, P. Zhou, Endocytosis mechanism of a novel proteoglycan, extracted from Ganoderma lucidum, in HepG2 cells, RSC Advances 7(66) (2017) 41779-41786.
[13] S.-K. Eo, Y.-S. Kim, C.-K. Lee, S.-S. Han, Antiherpetic activities of various protein bound polysaccharides isolated from Ganoderma lucidum, J. Ethnopharmacol. 68(1) (1999) 175-181.
[14] P. Saard, R. Sarnthima, S. Khammuang, W. Kanchanarach, Antioxidant, antibacterial and DNA protective activities of protein extracts from Ganoderma lucidum, Journal of Food Science &

DPPH and ABTS Assays to Assess the Antioxidant Profile of Untreated Oils, Food Analytical Methods 8(5) (2014) 1-9.
[18] B. Yang, M. Zhao, P. Knagendra, G. Jiang, Y. Jiang, Effect of methylation on the structure and radical scavenging activity of polysaccharides from longan (Dimocarpus longan Lour.) fruit pericarp, Food. Chem. 118(2) (2010) 364-368.
[19] W.Y. Zhang, J.-J. Lee, I.-S. Kim, Y. Kim, J.-S. Park, C.-S. Myung, 7-O-Methylaromadendrin Stimulates Glucose Uptake and Improves Insulin Resistance in Vitro, Biol. Pharm. Bull. 33(9) (2010) 1494-1499.
[20] W. Cui, L. Cheng, H. Li, Y. Zhou, Y. Zhang, J. Chang, Preparation of hydrophilic poly(l -lactide) electrospun fibrous scaffolds modified with chitosan for enhanced cell biocompatibility, Polymer. 53(11) (2012) 2298-2305.
[21] B. He, H. Tao, A. Wei, S. Liu, X. Li, R. Chen, Protection of carboxymethylated chitosan on chondrocytes from nitric oxide-induced apoptosis by regulating phosphatidylinositol 3-kinase/Akt signaling pathway, Biochem Biophys Res Commun 479(2) (2016) 380-386.
[22] S.N. Kulikov, S.A. Lisovskaya, P.V. Zelenikhin, E.A. Bezrodnykh, D.R. Shakirova, I.V. Blagodatskikh, V.E. Tikhonov, Antifungal activity of oligochitosans (short chain chitosans) against some Candida species and clinical isolates of Candida albicans : Molecular weight–activity relationship, Eur. J. Med. Chem. 74(3) (2014) 169-178.
[23] D.-Y. Zhang, Y. Wan, J.-Y. Xu, G.-H. Wu, L. Li, X.-H. Yao, Ultrasound extraction of polysaccharides from mulberry leaves and their effect on enhancing antioxidant activity, Carbohydr. Polym. 137 (2016) 473-479.
[24] C. Chen, L.J. You, A.M. Abbasi, X. Fu, R.H. Liu, Optimization for ultrasound extraction of polysaccharides from mulberry fruits with antioxidant and hyperglycemic activity in vitro, Carbohydr. Polym. 130 (2015) 122-32.
[25] M.E.M. Braga, S.R.M. Moreschi, M.A.A. Meireles, Effects of supercritical fluid extraction on Curcuma longa L. and Zingiber officinale R. starches, Carbohydr. Polym. 63(3) (2006) 340-346.
[26] R.E. Poms, C. Capelletti, E. Anklam, Effect of roasting history and buffer composition on peanut protein extraction efficiency, Mol. Nutr. Food. Res. 48(6) (2004) 459-64.
[27] Y. Huangfu, K. Ruan, H. Qiu, Y. Lu, C. Liang, J. Kong, J. Gu, Fabrication and investigation on the PANI/MWCNT/thermally annealed graphene aerogel/epoxy electromagnetic interference shielding nanocomposites, Composites Part A: Applied Science and Manufacturing 121 (2019) 265-272.
[28] C. Liang, H. Qiu, Y. Han, H. Gu, P. Song, L. Wang, J. Kong, D. Cao, J. Gu, Superior electromagnetic interference shielding 3D graphene nanoplatelets/reduced graphene oxide foam/epoxy nanocomposites with high thermal conductivity, Journal of Materials Chemistry C 7(9) (2019) 2725-2733.
[29] L. Wang, L. Chen, P. Song, C. Liang, Y. Lu, H. Qiu, Y. Zhang, J. Kong, J. Gu, Fabrication on the

[32] Q. Li, N. Yu, Y. Wang, Y. Sun, K. Lu, W. Guan, Extraction optimization of Bruguiera gymnorrhiza polysaccharides with radical scavenging activities, Carbohydr. Polym. 96(1) (2013) 148-155.
[33] J.R. Al-Obaidi, N.B. Saidi, S.R. Usuldin, S.N. Hussin, N.M. Yusoff, A.S. Idris, Comparison of Different Protein Extraction Methods for Gel-Based Proteomic Analysis of Ganoderma spp, Protein. J. 35(2) (2016) 100-6.
[34] M.P. Colombin, A. Ceccarini, A. Carmignani, Ion chromatography characterization of polysaccharides in ancient wall paintings, J. Chromatogr. A. 968(1–2) (2002) 79-88.
[35] V.U. Girjal, S. Neelagund, M. Krishnappa, Antioxidant Properties of the Peptides Isolated From Ganoderma lucidum Fruiting Body, Int. J. Pept. Res. Ther. 18(4) (2012) 319-325.
[36] D. Lious, L. Fogelfeld, A. Amblee, Combination of Saxagliptin and Metformin Is Effective as Initial Therapy in New-Onset Type 2 Diabetes Mellitus With Severe Hyperglycemia, The Journal of Clinical Endocrinology & Metabolism 101(6) (2016) 2528-2535.
[37] G. Liu, Z. Xin, H. Liang, C. Abadzapatero, P.J. Hajduk, D.A. Janowick, B.G. Szczepankiewicz, Z. Pei, C.W. Hutchins, S.J. Ballaron, Selective protein tyrosine phosphatase 1B inhibitors: targeting the second phosphotyrosine binding site with non-carboxylic acid-containing ligands, J. Med. Chem. 46(16) (2003) 3437-40.
[38] M.G. Ignatova, N.E. Manolova, R.A. Toshkova, I.B. Rashkov, E.G. Gardeva, L.S. Yossifova, M.T. Alexandrov, Electrospun Nanofibrous Mats Containing Quaternized Chitosan and Polylactide with In Vitro Antitumor Activity against HeLa Cells, Biomacromolecules. 11(6) (2010) 1633-1645.
[39] W.A. Elkhateeb, G.M. Zaghlol, I.M. Elgarawani, E.F. Ahmed, M.E. Rateb, A.M. Abdel, Ganoderma applanatum secondary metabolites induced apoptosis through different pathways: In vivo and in vitro anticancer studies, Biomedicine & pharmacotherapy = Biomedecine & pharmacotherapie 101 (2018) 264-277.
[40] X.L. Zhu, A.F. Chen, Z.B. Lin, Ganoderma lucidum polysaccharides enhance the function of immunological effector cells in immunosuppressed mice, J. Ethnopharmacol. 111(2) (2007) 219-226.
[41] S.J. Chen, H.H. Lin, W.C. Huang, P.J. Tsai, W.P. Chen, D.C. Chen, L.T. Chuang, Ling-Zhi-8 protein (LZ-8) suppresses the production of pro-inflammatory mediators in murine microglial BV-2 cells, Food. Agric. Immunol. 28(6) (2017) 1393-1407.
[42] H. Wang, T.B. Ng, Ganodermin, an antifungal protein from fruiting bodies of the medicinal mushroom Ganoderma lucidum, Peptides. 27(1) (2006) 27-30.
[43] L.F. Zhu, Z.C. Yao, Z. Ahmad, J.S. Li, M.W. Chang, Synthesis and Evaluation of Herbal Chitosan from Ganoderma Lucidum Spore Powder for Biomedical Applications, Sci. Rep. 8(1) (2018) 14608.
[44] I.C.F.R. Ferreira, S.A. Heleno, F.S. Reis, D. Stojkovic, M.J.R.P. Queiroz, M.H. Vasconcelos, M. Sokovic, Chemical features of Ganoderma polysaccharides with antioxidant, antitumor and antimicrobial activities, Phytochemistry. 114 (2015) 38-55.
[45] F. He, Y. Yang, G. Yang, L. Yu, Studies on antibacterial activity and antibacterial mechanism of

Fig. 1. Contour plots (2D) for response surface plots results: a-f corresponding to temperature and time, pH and temperature, pH and time, time and solid-to-liquid ratio, pH and solid-to-liquid-ratio, temperature and solid-to-liquid ratio, respectively.

Fig. 2. FT-IR spectroscopy of proteoglycan (a) and SDS-PAGE of crude protein contained in proteoglycan (b): lane 1, molecular weight markers; lane 2-4, proteoglycan-C in triplicate; lane 5-7, proteoglycan-UC in triplicate.

Fig. 3. Amino acids content of proteoglycan-UC (a) and proteoglycan-C (b); monosaccharides content of proteoglycan-UC (c) and proteoglycan-C (d).

Fig. 4. The antioxidant effects of proteoglycan-C and proteoglycan-UC.

Fig. 5. The hypoglycemic capacity against normal HepG2 cells (a) and insulin resistance type HepG2 cells (b) of proteoglycan.

Fig. 6. Effects of proteoglycan on HeLa cell viability using CCK-8 assay (a); Fluorescent images of HeLa cells morphology of blank control group (b) and treated with proteoglycan-C of 1.0 mg/mL (b1), 0.5 mg/mL (b2) and proteoglycan-UC of 1.0 mg/mL (c1), 0.5 mg/mL (c2).

Fig. 7. Effects of proteoglycan on HeLa cell viability using CCK-8 assay (a); and on proliferation of *E. coli* (a) and *S. aureus* (b); inhibition zone results of proteoglycan-UC (c1, d1) and proteoglycan-C (c2, d2) against *E. coli* (c1, c2) and *S. aureus* (d1, d2).

	Inhibition zone diameter (Φ, mm)	
	Proteoglycan-UC	Proteoglycan-C
E. coli	20.1	20.8
S. aureus	25.2	27.2

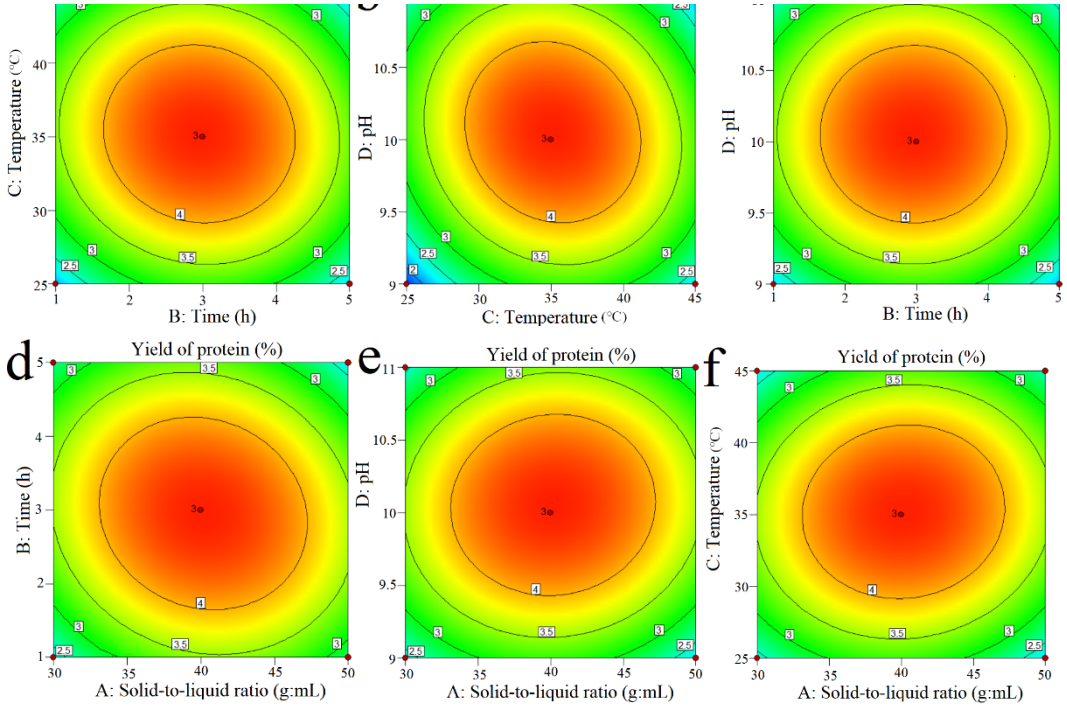
C: Temperature (°C)
B: Time (h)
D: pH
C: Temperature (°C)
D: pH
B: Time (h)
d
Yield of protein (%)
B: Time (h)
A: Solid-to-liquid ratio (g:mL)
e
Yield of protein (%)
D: pH
A: Solid-to-liquid ratio (g:mL)
f
Yield of protein (%)
C: Temperature (°C)
A: Solid-to-liquid ratio (g:mL)

Fig. 1

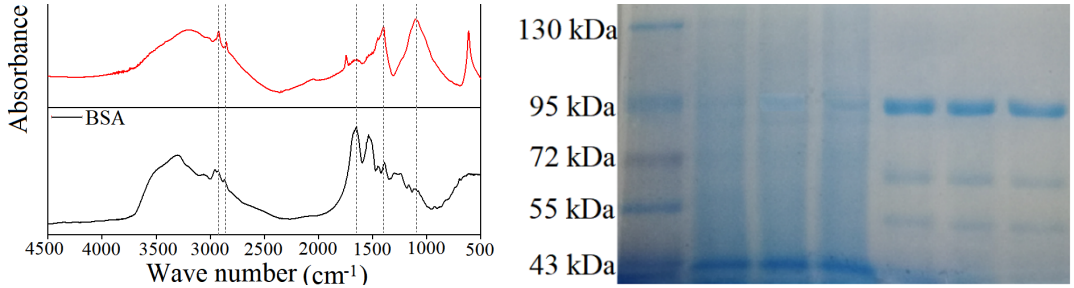
Absorbance
BSA
4500 4000 3500 3000 2500 2000 1500 1000 500
Wave number (cm-1)
130 kDa
95 kDa
72 kDa
55 kDa
43 kDa

Fig. 2

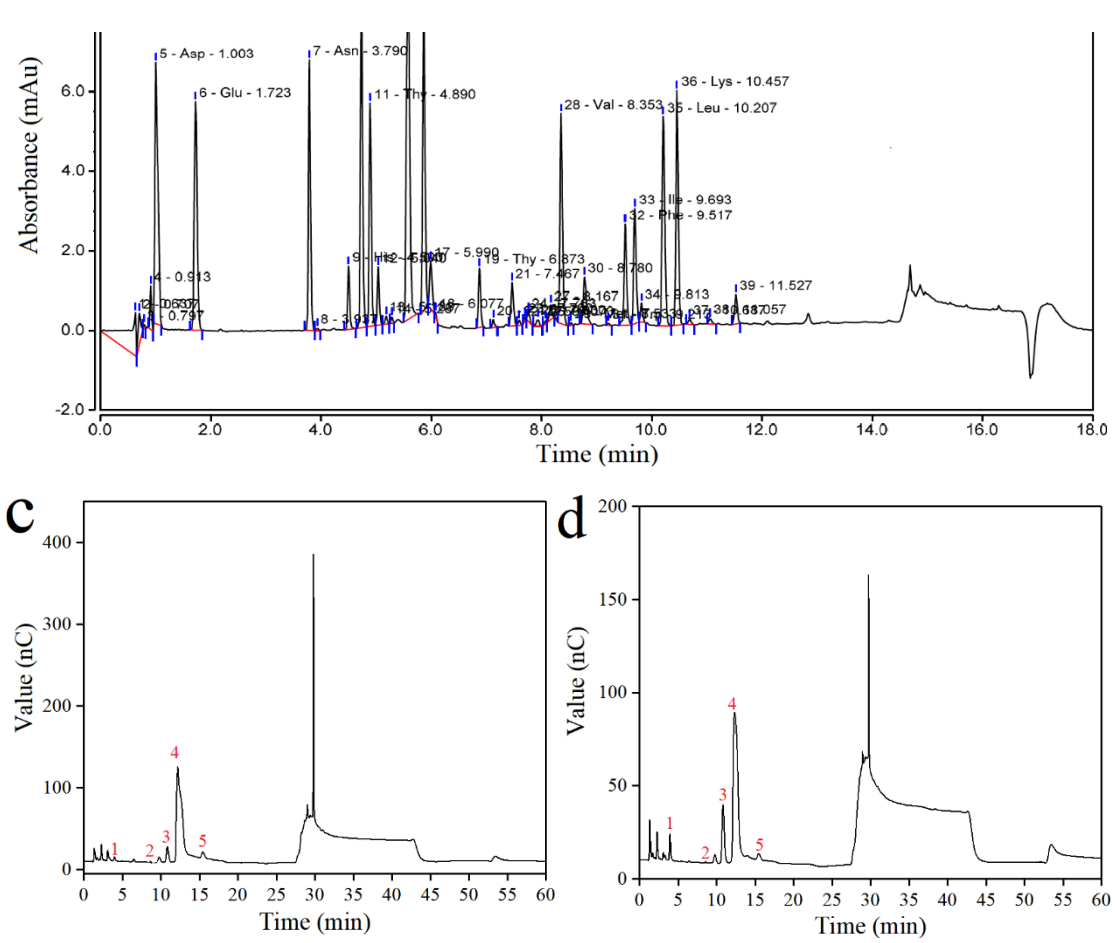
5 - Asp - 1.003
7 - Asn - 3.790
6 - Glu - 1.723
11 - Thr - 4.890
36 - Lys - 10.457
28 - Val - 8.353
35 - Leu - 10.207
33 - Ile - 9.693
32 - Phe - 9.517
19 - Thr - 6.873
21 - 7.467
30 - 8.780
39 - 11.527
Absorbance (mAu)
Time (min)
c
Value (nC)
Time (min)
d
Value (nC)
Time (min)

Fig. 3.

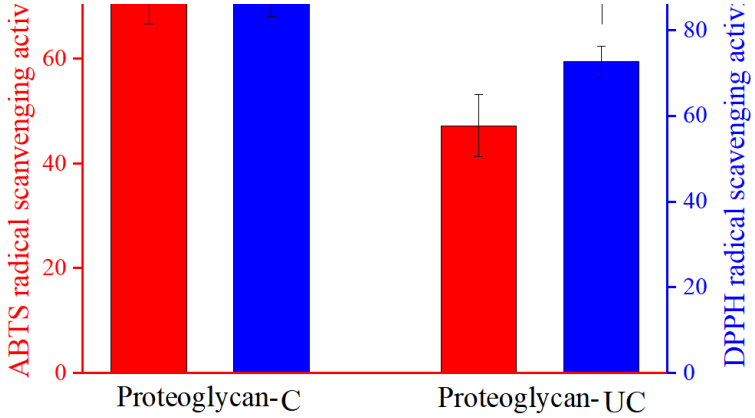
ABTS radical scanvenging activ
DPPH radical scavenging activ
0
20
40
60
80
Proteoglycan-C
Proteoglycan-UC

Fig. 4

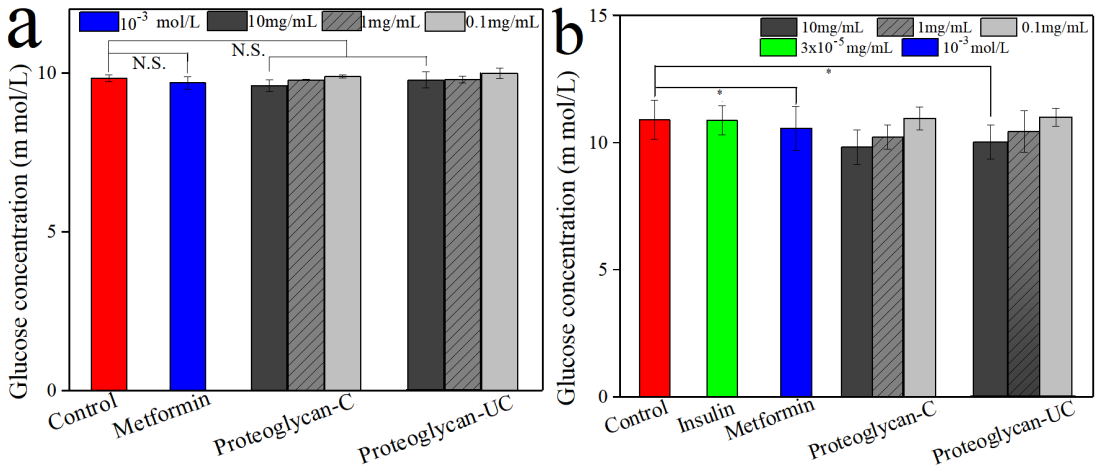
a
b
Glucose concentration (m mol/L)
10^-3 mol/L
10mg/mL
1mg/mL
0.1mg/mL
3x10^-5 mg/mL
N.S.
*
Control
Insulin
Metformin
Proteoglycan-C
Proteoglycan-UC

Fig. 5

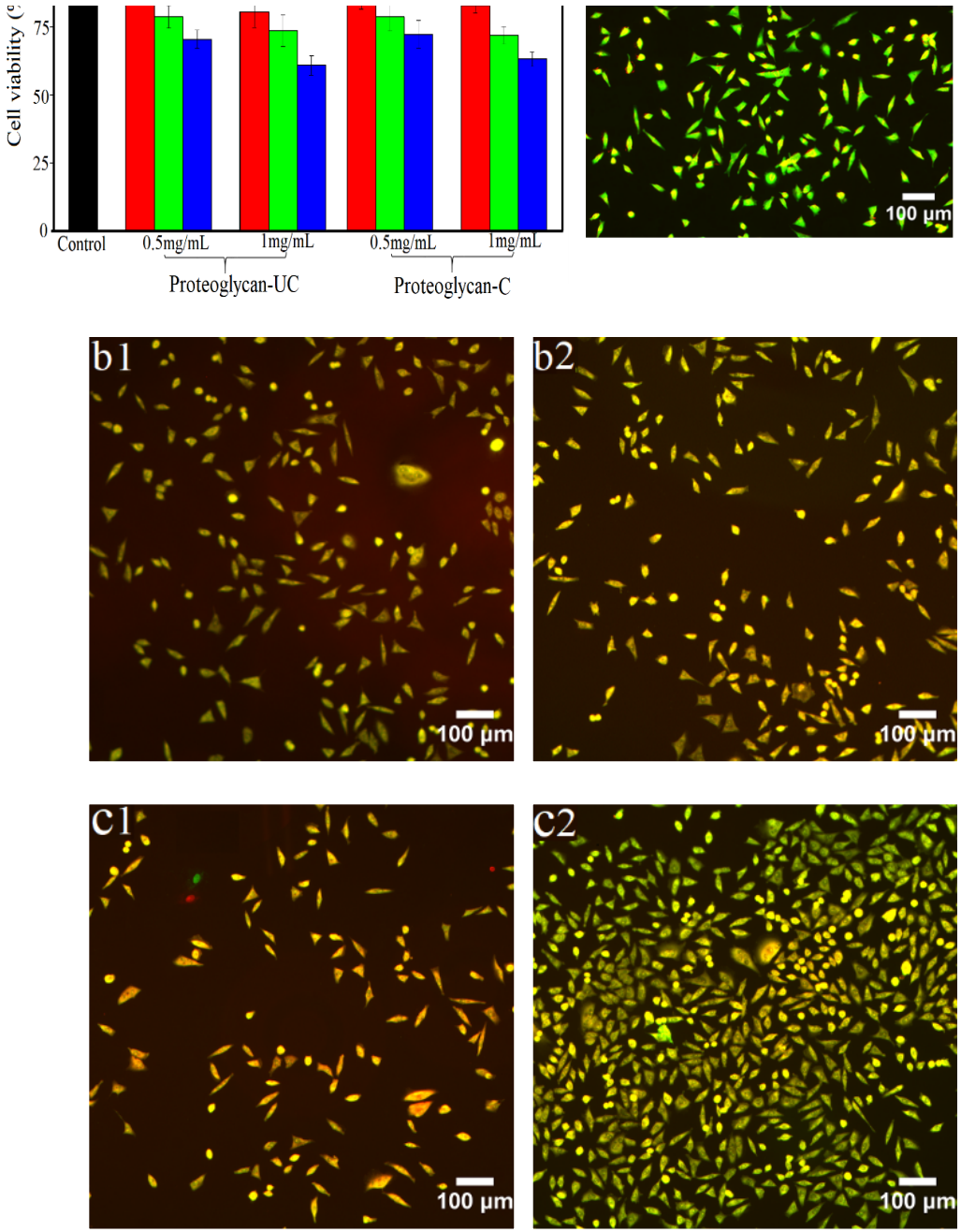
Cell viability (%
75
50
25
0
Control
0.5mg/mL
1mg/mL
0.5mg/mL
1mg/mL
Proteoglycan-UC
Proteoglycan-C
100 μm
b1
100 μm
b2
100 μm
c1
100 μm
c2
100 μm

Fig. 6

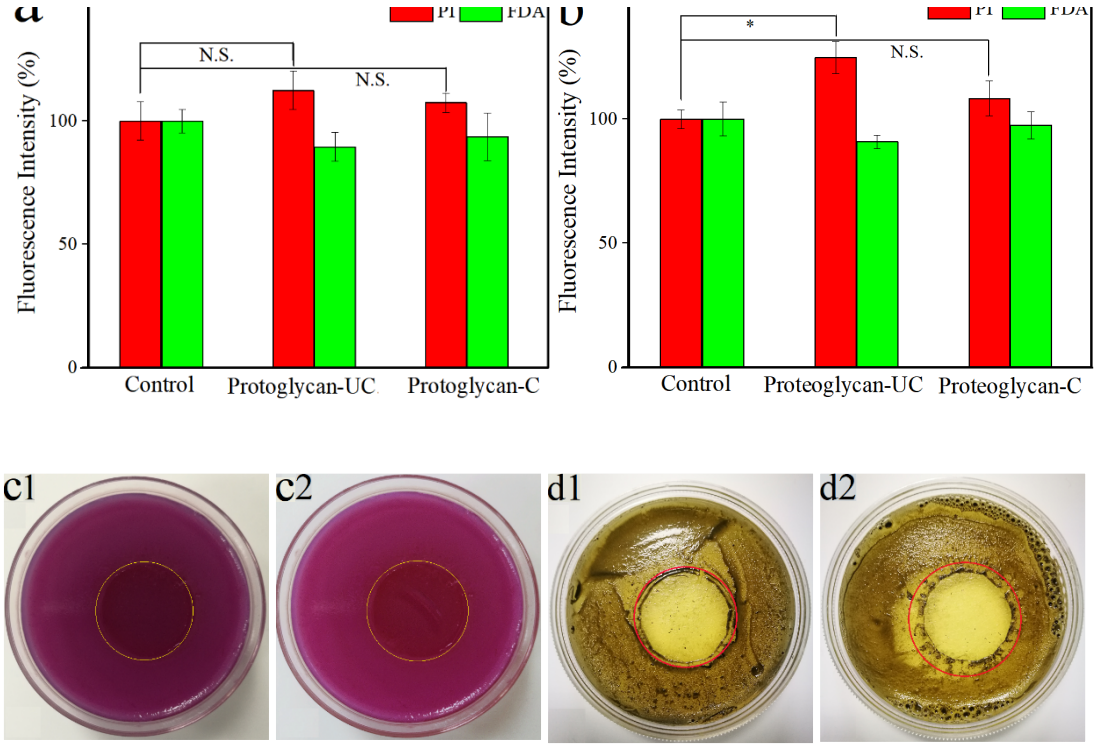
a
PI
FDA
Fluorescence Intensity (%)
100
50
0
N.S.
N.S.
Control
Protoglycan-UC
Protoglycan-C
b
PI
FDA
Fluorescence Intensity (%)
100
50
0
*
N.S.
Control
Proteoglycan-UC
Proteoglycan-C
c1
c2
d1
d2

Fig. 7